

Confinement, enhancement, extremes and inversions in the mixing and transport of particles by rotating turbulent flows

By A.D. Bragg[†] AND R. Dhariwal[†]

In this study, we investigate using theory and Direct Numerical Simulations (DNS) in the multiscale mixing and transport of inertial particles in rotating turbulent flows. The goal of this work is to understand how the direct and indirect effects of rotation on the particle dynamics compete and control the particle motion. We consider the relative dispersion of both fluid and inertial particles in the directions normal and perpendicular to the rotation axis. We also derived theoretical predictions for the particle dispersion in the direction normal to the rotation axis using Zeman phenomenology, and present new insights concerning some of the subtle effects of rotation on the particle-pair motion. Our DNS results for the mean-square separation of fluid particles are found not to be in agreement with the theoretical predictions. This is in part due to limited Zeman scaling for the fluid velocity increments in our DNS due to the moderate Reynolds number. However, we argue that it may be also due to rotation leading to strongly non-monotonic behavior in the Lagrangian autocorrelations of the fluid velocity increments. We also observe that the implicit effect of rotation on the inertial particle motion causes their relative dispersion to become slower with increasing particle inertia. This is exactly the opposite to the non-rotating case, where particle inertia is known to strongly enhance small-scale relative dispersion due to the effect of caustics.

1. Introduction

The effect of rotation on turbulence is of great importance to geophysical, astrophysical, and industrial flows (Davidson 2013). Many of these flows also contain small, suspended particles, often with inertia, and understanding the effect of the rotating turbulence on their mixing and transport can be very consequential. The rotation of the Earth is expected to affect the transport and mixing of pollutants and aerosols in the atmosphere (Csanady 1973), along with the vertical transport and mixing of particulate matter in the ocean (Rotunno & Bryan 2012). The subject is also important for designing effective cyclone dust particle collectors (Balestrin *et al.* 2017).

The effect of rotation on turbulence is a complex problem that has long been studied, and it continues to be a very active area of research because of the many fundamental problems that remain to be solved. On the other hand, despite its importance in the aforementioned applications, the problem of particle motion in rotating turbulent flows has received little attention. Recent results (Biferale *et al.* 2016) show that rotation strongly affects turbulence not only at the large scales, but even down to the smallest scales, strongly suggesting that rotation could impact the mixing and transport of particles at all scales of the flow. However, this effect has barely been investigated, and hence the current study aims to help elucidate these knowledge gaps.

[†] Department of Civil and Environmental Engineering, Duke University

1.1. How rotation affects turbulence

We are concerned with homogeneous, rotating turbulence in incompressible, Newtonian fluids, far from boundaries. In the rotating frame of reference, the effect of rotation on the fluid dynamics is through Coriolis and centrifugal forces. The importance of these forces on the flow depends upon the strength of the rotation, quantified through the Rossby number, $Ro \equiv U/L\Omega$, where U, L are characteristic velocity and lengthscales, and Ω is the rotation frequency. The Rossby number can be thought of as a ratio between the rotation timescale $\tau_\Omega \equiv 1/\Omega$, and the turbulent timescale L/U . When $Ro \leq O(1)$, rotation has a strong effect on the turbulent motions of the fluid.

It is also informative to consider how τ_Ω compares with τ_r , the eddy turnover timescale for a scale of motion of size r . The scale at which $\tau_\Omega = \tau_r$ is the Zeman scale r_Ω (Zeman 1994). At scales $r > r_\Omega$, rotation strongly affects the turbulent motions, leading to the formation of quasi-2D coherent columnar vortices aligned with the rotation axis. At scales $r < r_\Omega$, the turbulent motions are fully 3D, and in contrast to expectations based upon simple scaling arguments, the effect of rotation is evident even at scales much smaller than r_Ω . A very interesting and consequential result in Biferale *et al.* (2016) is that although the intermittency of the overall turbulent velocity field is reduced with increasing rotation, the non-Gaussianity of the velocity fluctuations (indicated by deviations of the scale-dependent kurtosis from 3) of the flow was significantly enhanced.

1.2. How rotation affects particle motion in turbulence

There has been a significant advance in the understanding of how various kinds of particles move in turbulent flows, especially isotropic flows (Toschi & Bodenschatz 2009). Yet, despite its great practical importance, very little is known concerning how rotation affects the motion of particles in turbulence. In principle, rotation can affect particle motion in turbulence in two ways: 1) explicitly, through the introduction of Coriolis and centrifugal forces on the particles, and 2) implicitly, by modifying the behavior and spatio-temporal structure of the turbulent velocity field that transports the particles.

In Del Castello & Clercx (2011), the acceleration of fluid particles (tracers) in statistically stationary, homogeneous rotating turbulence was investigated. These authors showed that strong accelerations of the fluid particles in the direction parallel to the rotation axis are suppressed with increasing Ω , whereas they are strongly enhanced in the direction normal to the rotation axis. In Elperin *et al.* (1998), the effect of rotation on particle motion in turbulence was analyzed theoretically. They predicted that when the mean helicity of fluid flow is finite, it generates an additional flux mechanism for inertial particle transport along the direction parallel to the rotation axis. However, their analysis is limited to the case of weakly inertial particles. It is only very recently that more comprehensive investigations have been undertaken. In Biferale *et al.* (2016), high-resolution DNS was used to study the transport of heavy and light (density greater than and less than that of the fluid, respectively) point-particles. Their results showed that rotation can have a dramatic effect on particle transport in turbulence. For example, they showed that rotation leads to extreme preferential sampling due to the columnar coherent structures in the flow. In Biferale *et al.* (2016) they show that this extreme preferential sampling leads to a dramatic effect on the large-scale particle mixing; heavy particles mix more efficiently in the plane normal to the rotation axis, whereas the light particles tend to mix only along the direction parallel to the rotation axis. This finding could have dramatic implications for understanding how suspensions of particles of varying density mix in rotating flows, with many natural and industrial applications.

These preliminary investigations show that rotation can have strong and non-trivial effects on particle motion in turbulence. However, many crucial questions remain to be solved, and solving these is the aim of our current work.

The remainder of this report is structured as follows. In Section 2, the computational setup is briefly outlined. Section 3 is devoted to the theoretical analysis. Section 4 is focused on the results obtained in this study. Finally, conclusions are drawn in Section 5.

2. Direct numerical simulations

2.1. Fluid phase

We consider the evolution of an incompressible fluid velocity field \mathbf{u} , in a frame of reference rotating with constant angular frequency Ω , governed by the Navier-Stokes Equation

$$\partial_t \mathbf{u} + (\mathbf{u} \cdot \nabla) \mathbf{u} + 2\boldsymbol{\Omega} \times \mathbf{u} = -(1/\rho^f) \nabla p + \nu \nabla^2 \mathbf{u} + (1/\rho^f) \mathbf{F}, \quad (2.1)$$

where ρ^f, ν are the fluid density and kinematic viscosity, respectively, $\boldsymbol{\Omega}$ is the rotation vector (with $\boldsymbol{\Omega} \equiv \mathbf{e}_\Omega \Omega$, $\Omega \equiv \|\boldsymbol{\Omega}\|$), $2\boldsymbol{\Omega} \times \mathbf{u}$ is the Coriolis force, p is the fluid pressure (determined via $\nabla \cdot \mathbf{u} = 0$), and \mathbf{F} is an external force.

Our DNS code uses a pseudospectral approach, and the P3DFFT library (Pekurovsky 2012) is used to carry out the transforms between physical and spectral spaces. Time integration is performed using a second-order, explicit Runge-Kutta scheme with aliasing errors removed using a combination of spherical truncation and phase-shifting. In order to generate statistically stationary turbulence, a deterministic forcing method is employed for \mathbf{F} that re-injects energy dissipated in a given timestep into wavenumbers k_f . We choose $k_f \in [4, 6]$ so that small scales of the turbulence are weakly affected by the forcing, with enough spectral room for the large scales to develop an inverse energy cascade when $Ro < 1$. When an inverse energy cascade occurs, energy will pile up at the large scales of the system, and a statistically stationary state will not be obtained. We adopt the method proposed by Biferale *et al.* (2016), which is to remove energy at the large scales by adding a linear friction term $\alpha \nabla^{-2} \mathbf{u}$ to the NSE, that only acts on wavenumbers $k \leq 2$, with α chosen to achieve a stationary state. Our simulations are based on a grid resolution 512^3 with a domain length 2π , and in the non-rotating case the DNS parameters give $R_\lambda \approx 225$, with $k_{max}\eta \approx 1.6$. In the presence of rotation, the Kolmogorov scales increase due to a suppression of the downscale energy cascade.

2.2. Particle phase

In the rotating flow, we will consider the motion of fluid and inertial particles. In many of the motivating applications, the particle loading is dilute and the fluid-particle flow is “one-way coupled”. Particles with diameter d_p and density ρ_p are often well described in these problems as being small, i.e., $d_p \ll \eta$, where η the Kolmogorov lengthscale, and “heavy”, i.e., $\rho_p/\rho_f \gg 1$. As such, the motion of the particles is described well by a simplified form of the Maxey & Riley equation (Maxey & Riley 1983), which, when written in the rotating frame of reference, is (ignoring gravity)

$$\frac{d^2}{dt^2} \mathbf{x}^p(t) \equiv \frac{d}{dt} \mathbf{v}^p(t) = \frac{\mathbf{u}(\mathbf{x}^p(t), t) - \mathbf{v}^p(t)}{\tau_p} - 2\boldsymbol{\Omega} \times \mathbf{v}^p(t) - \boldsymbol{\Omega} \times \left[\boldsymbol{\Omega} \times (\mathbf{x}^p(t) - \mathbf{x}_0) \right], \quad (2.2)$$

where $\mathbf{x}^p(t), \mathbf{v}^p(t)$ are the particle position and velocity, respectively, $\mathbf{u}(\mathbf{x}^p(t), t)$ is the fluid velocity at the particle position, and τ_p is the particle momentum response time.

The terms on the right-hand side are Stokes drag, Coriolis, and centrifugal accelerations (\mathbf{x}_0 is the location of the rotation axis), respectively. In our DNS, Eq. (2.2) is solved using a modified RK2 method in which the standard RK2 weights are replaced by exponential integrators (Ireland *et al.* 2013). Further, $\mathbf{u}(\mathbf{x}^p(t), t)$ is obtained using an 8th order B-spline scheme to interpolate the fluid velocities at the grid points to the particle position.

In our simulations, 262144 particles were tracked, and after their statistics had reached steady state, their statistics were recorded over a duration of 15 large-eddy turnover times.

3. Theoretical considerations and results

For two physically identical inertial particles whose motion is governed by Eq. (2.2), the equation governing their relative motion is

$$\mathbf{w}^p(t) = \Delta\mathbf{u}^p(t) - \tau_p\dot{\mathbf{w}}^p(t) - 2\tau_p\Omega\left[\mathbf{e}_\Omega \times \mathbf{w}^p(t)\right] - \tau_p\Omega^2\mathbf{e}_\Omega \times \left[\mathbf{e}_\Omega \times \mathbf{r}^p(t)\right], \quad (3.1)$$

where $\mathbf{w}^p(t)$ is the particle-pair relative velocity, $\mathbf{r}^p(t)$ is their separation, $\Delta\mathbf{u}^p(t)$ is the difference in the fluid velocity at the positions of the two particles. According to Eq. (3.1), the relative motion of particle-pairs is affected by rotation explicitly through the Coriolis and centrifugal forces, and implicitly through the effect of rotation on $\Delta\mathbf{u}^p(t)$.

It is helpful to introduce the scale-dependent Rossby number $Ro_r \equiv 1/(\tau_r\Omega)$, where τ_r is the turnover timescale for a scale of size r . If we, in addition, introduce the scale-dependent Stokes number $St_r \equiv \tau_p/\tau_r$, then we may non-dimensionalize Eq. (3.1) to obtain (omitting \sim on non-dimensionalized variables for notational ease)

$$\mathbf{w}^p(t) = \Delta\mathbf{u}^p(t) - St_r\dot{\mathbf{w}}^p(t) - \frac{2St_r}{Ro_r}\left[\mathbf{e}_\Omega \times \mathbf{w}^p(t)\right] - \frac{St_r}{Ro_r^2}\mathbf{e}_\Omega \times \left[\mathbf{e}_\Omega \times \mathbf{r}^p(t)\right]. \quad (3.2)$$

Typically, in atmospheric contexts, $Ro \geq O(0.1)$, such that with the large Reynolds number of atmospheric flows, strong effects of rotation on the particle transport will only be felt down to scales in the upper portion of the inertial range of the turbulence. However, in industrial and engineered contexts, both Ro and/or R_λ can be much smaller, implying that the effects of rotation may be felt across a much larger range of scales.

3.1. Sweeping the particle-pair center of mass

We now explain a new effect that seems not to have been previously identified, but which could be important for inertial particle transport in rotating turbulent flows.

Even at scales where $St_r/Ro_r^2 \ll 1$, it is possible for the centrifugal force to implicitly affect the relative motion of inertial particles in turbulence. In particular, the centrifugal force can cause the center of mass of the particle-pair to be swept through turbulent eddies of size corresponding to $St_r/Ro_r^2 \ll 1$, modifying how the particles interact with these scales. To see this, note that $\Delta\mathbf{u}^p(t) \equiv \Delta\mathbf{u}[\mathbf{x}^p(t), \mathbf{r}^p(t), t]$, where $\mathbf{x}^p(t)$ can be considered the center of mass of the particle pair, and $\mathbf{r}^p(t)$ the separation between the particles. The center of mass obeys $\mathbf{v}^p(t) \equiv \dot{\mathbf{x}}^p(t)$, and by normalizing Eq. (2.2) by the large-scale variables and re-arranging we obtain

$$\mathbf{v}^p(t) = \mathbf{u}^p(t) - St_\ell\dot{\mathbf{v}}^p(t) - \frac{2St_\ell}{Ro}\left[\mathbf{e}_\Omega \times \mathbf{v}^p(t)\right] - \frac{St_\ell}{Ro^2}\mathbf{e}_\Omega \times \left[\mathbf{e}_\Omega \times (\mathbf{x}^p(t) - \mathbf{y})\right], \quad (3.3)$$

where $St_\ell \equiv \tau_p/\tau_\ell$ denotes the large-scale Stokes number (τ_ℓ is the integral timescale), and \mathbf{y} is the location of the rotation axis. Even if $St_\ell \ll 1$, the centrifugal term can play a leading order role in Eq. (3.3) when $Ro \ll 1$, if $\|\mathbf{x}^p(t) - \mathbf{y}\| \geq O(1)$. To estimate

the importance of this effect, we can re-write Eq. (3.3) by using the standard scaling $\tau_\ell/\tau_\eta \sim Re^{1/2}$ with $R_\lambda = \sqrt{15Re}$ to obtain

$$\mathbf{v}^p(t) = \mathbf{u}^p(t) - \frac{\sqrt{15}St}{R_\lambda} \dot{\mathbf{v}}^p(t) - \frac{2\sqrt{15}St}{RoR_\lambda} \left[\mathbf{e}_\Omega \times \mathbf{v}^p(t) \right] - \frac{\sqrt{15}St}{Ro^2R_\lambda} \mathbf{e}_\Omega \times \left[\mathbf{e}_\Omega \times (\mathbf{x}^p(t) - \mathbf{y}) \right]. \quad (3.4)$$

If we take $St = 1$ and $R_\lambda = 10^3$, then for $\|\mathbf{x}^p(t) - \mathbf{y}\| = O(1)$ (particle distance from the rotation axis is of the order of the integral length scale ℓ), the centrifugal term is $O(1)$ for $Ro = O(10^{-1})$, which is certainly within the regime of practical interest in industrial contexts. For these same values, the Kolmogorov scale Rossby number is $Ro_\eta \approx 25$ so that the explicit effect of rotation on the particle-pair motion in the dissipation range is negligible. However, implicitly, their dissipation range motion would still be strongly affected by rotation since the motion of their center of mass would be strongly affected by the centrifugal force, modifying $\Delta\mathbf{u}^p(t)$, and leading to a reduction in the correlation timescales of $\Delta\mathbf{u}^p(t)$ as particle-pairs are pulled through the small-scale turbulent eddies by the centrifugal force acting on their center of mass. This effect is somewhat analogous to the effect of gravity that also reduces the timescales of $\Delta\mathbf{u}^p(t)$ (Ireland *et al.* 2016).

In natural contexts, such as atmospheric flows, this effect may not be important as there one would typically expect $St/Ro^2R_\lambda \ll 1$. It may be of importance for the atmospheric transport of larger hydrometeors (e.g., hail) with large St ; however this requires further investigation, and its analysis could not be based on Eq. (2.2).

3.2. Particle-pair dispersion predictions

Although it is possible to derive rigorous results for particle dispersion in turbulence using Probability Density Function (PDF) phase-space equations (e.g., Bragg *et al.* (2012)), we first consider simple, phenomenological approaches, based on the ideas of Richardson (1926), modified to account for the effects of rotation and particle inertia. In Richardson's seminal work (Richardson (1926)), he assumed that the PDF of the particle-pair separation $\mathcal{P}(r, t)$ obeys a diffusion equation with a scale-dependent diffusion coefficient $\mathcal{D}(r) \propto r^{4/3}$. This modeling procedure assumes that the dispersion process is isotropic; however, in rotating turbulence, this relative dispersion is anisotropic at scales affected by rotation. Homogeneous rotating turbulence is axisymmetric, and the expectation is that particle motion at scales strongly affected by rotation will be quasi-2D, with dispersion in the direction \mathbf{e}_Ω being strongly suppressed compared to that in the plane normal to \mathbf{e}_Ω . In view of these considerations, we may model the particle-pair dispersion by an isotropic diffusion equation in the 2D plane normal to \mathbf{e}_Ω

$$\partial_t \mathcal{P} = r^{-1} \nabla_r \left(r \mathcal{D} \nabla_r \mathcal{P} \right). \quad (3.5)$$

In order to account for the effects of particle inertia on the diffusion coefficient \mathcal{D} , we appeal to results from phase-space PDF equations that show that for inertial particles, \mathcal{D} is comprised of two parts, one from the turbulence and another from the particle velocities themselves, the latter dominating in the regime of ballistic particle motion (Zaichik & Alipchenkov (2009); Bragg (2017)). For diffusion in the 2D plane we have $\mathcal{D}(r) = -\tau_p(\lambda_\perp + \langle w_\perp^p(t) w_\perp^p(t) \rangle_r)$, where λ_\perp is the contribution from the fluid velocity increments in the plane normal to \mathbf{e}_Ω , and $\langle w_\perp^p(t) w_\perp^p(t) \rangle_r$ is the second-order structure function for the inertial particle relative velocities in the plane normal to \mathbf{e}_Ω , conditioned on their separation satisfying $\|\mathbf{r}^p(t)\| = r$. Analytic forms for $\langle w_\perp^p(t) w_\perp^p(t) \rangle_r$ for arbitrary r and St are very difficult to construct [see Bragg & Collins (2014)]. Therefore, as a first

step we restrict attention to the regime $St_r = O(Ro_r^2)$, and $Ro_r \ll 1$, i.e., scales at which the effects of particle inertia are very weak and those of rotation are strong.

Next, we invoke Zeman phenomenology to account for the effects of rotation on the inertial range turbulence, which predicts that the velocity increments scale as $\Delta u^N \propto r^{N/2}$ (Zeman 1994), in contrast to K41 scaling which would give $\Delta u^N \propto r^{N/3}$. The Zeman phenomenology is essentially an extension of K41 that includes the effects of rotation in the dynamical quantities used to form the dimensional predictions.

Using Zeman scaling, we obtain the final form of the model

$$\partial_t \mathcal{P} = r^{-1} \nabla_r \left(r \mathcal{D} \nabla_r \mathcal{P} \right), \quad (3.6)$$

$$\mathcal{D} \sim r^{3/2} + \frac{St_r^3}{Ro_r^4} r^2, \quad \text{for } St_r = O(Ro_r^2), \text{ and } Ro_r \ll 1. \quad (3.7)$$

We may also directly construct predictions for the moments of the relative dispersion using Zeman phenomenology, for various asymptotic regimes. In particular we obtain for dispersion in the plane normal to e_Ω

$$\langle r^N(t) \rangle_\xi \sim \begin{cases} t^{2N}, & \text{if } Ro_r \ll 1, St_\Omega \ll Ro_r \\ e^{St_\Omega N t / Ro_r}, & \text{if } Ro_r \ll 1, St_\Omega \gg Ro_r. \end{cases} \quad (3.8)$$

The first result should be compared with the result for non-rotating homogeneous turbulence, where K41 scaling would give $\langle r^N(t) \rangle_\xi \sim t^{3N/2}$, which is slower than the $\langle r^N(t) \rangle_\xi \sim t^{2N}$ predicted for rotating turbulence.

4. Results

In Figure 1 we show DNS results for the mean-square separation $\langle r^2(t) \rangle_\xi$ for fluid particles with initial separation $\xi \in [1, 2]\eta$. The mean-square separation in the directions parallel and perpendicular to the rotation axis is shown as separate curves. As anticipated, the results show that the dispersion in the parallel direction is significantly suppressed compared to the perpendicular and non-rotating case. This is caused by the large-scale, quasi-2D coherent vortices in the flow that are aligned with the rotation axis, along which the velocity field is approximately constant. In this parallel direction we observe an asymptotic behavior that is close to $\langle r^2(t) \rangle_\xi \sim t^{3/2}$. The behavior $\langle r^2(t) \rangle_\xi \sim t^{3/2}$ is faster than diffusive, suggesting the role of spatial structure in the velocity field. However, there is no known way to describe this non-trivial scaling theoretically since the Zeman phenomenology only describes the velocity increments in the direction perpendicular to the rotation axis, and no phenomenology is available for the parallel direction. Indeed, several complications arise in attempting to construct a phenomenology for this direction. For example, even within the large-scale quasi-2D vortices, there exist smaller scale structures whose velocities are approximately three dimensional. Since a purely 2D vortex in the parallel direction would give rise to no separation between the particles in the parallel direction, the observed parallel dispersion is due to both the smaller scale structures embedded within the large-scale vortices and also the regions of the flow in between these vortices, concerning which not much is known.

The results in Figure 1 show that in the perpendicular direction, the mean-square separation growth is slightly slower than in the non-rotating ($Ro = \infty$) case. Moreover, the growth is much slower than the prediction $\langle r^2(t) \rangle_\xi \sim t^4$ that we derived in Section 3 based on simple phenomenological arguments based on Zeman scaling. The results

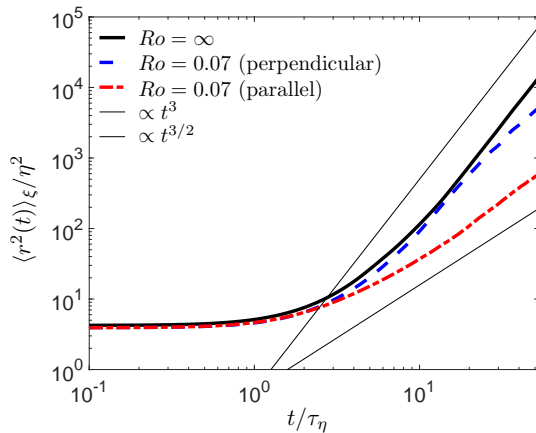


FIGURE 1. DNS results for $\langle r^2(t) \rangle_\xi$ for fluid particles with initial separation $\xi \in [1, 2]\eta$. The black solid line corresponds to the simulation without rotation, $Ro = \infty$, for which the dispersion is isotropic, and the blue dashed and red dashed-dot lines correspond to dispersion in the directions perpendicular and parallel to the rotation axis, respectively, for a flow with $Ro = 0.07$.

from our DNS for the fluid velocity structure functions show that this is due, at least in part, to deviations in the flow from Zeman scaling, which may be due to the moderate R_λ of our flow. Nevertheless, the scaling is still steeper than K41 scaling for the second order structure function, which under simple phenomenological arguments would lead to a mean-square dispersion that is faster than the Richardson prediction $\langle r^2(t) \rangle_\xi \sim t^3$, contrary to our DNS results in Figure 1.

One possible explanation for the strong deviation from theoretical predictions is that when fluid particles are trapped in the quasi-2D vortices, the autocorrelation of $\Delta \mathbf{u}^p(t)$ could exhibit strong negative loops. It is straightforward to show using known results on fluid particle dispersion (e.g., see results in Bragg *et al.* (2016)) that the presence of the negative loops would lead to a suppression of the separation rate of the particles. Simple phenomenological arguments do not account for such effects, which could be why they lead to significant overpredictions for the dispersion rate in rotating turbulent flows. We leave an examination of this effect to future work, where we will also consider larger R_λ to reach the regime where Zeman scaling is known to occur (Biferale *et al.* (2016)).

We now turn to consider results for the full dispersion PDF $\mathcal{P}(r, t)$ for fluid particles with initial separation $\xi \in [1, 2]\eta$. We plot the results in standard form in Figure 2 in order to look at the effects of rotation on extreme events in the pair dispersion process. The results indicate that rotation significantly suppresses extreme events in the dispersion in the parallel direction; however, there is no clear effect on the perpendicular dispersion. This is surprising given that it has been shown that rotation enhances the non-Gaussianity of fluid velocity increments in turbulence (Biferale *et al.* (2016)) which one would expect to lead to an enhancement in the extreme events of the fluid particle-pair dispersion. Again, the behavior may be due to the effect of the quasi-2D vortices on the temporal correlation structure of $\Delta \mathbf{u}^p(t)$.

Finally, we turn to the case of inertial particles. As explained earlier, rotation leads to an implicit and explicit effect on the inertial particle motion, and in order to understand the more subtle implicit effect, we have first conducted simulations in which the explicit effects of rotation on the particle motion are switched off (i.e., the Coriolis and centrifugal

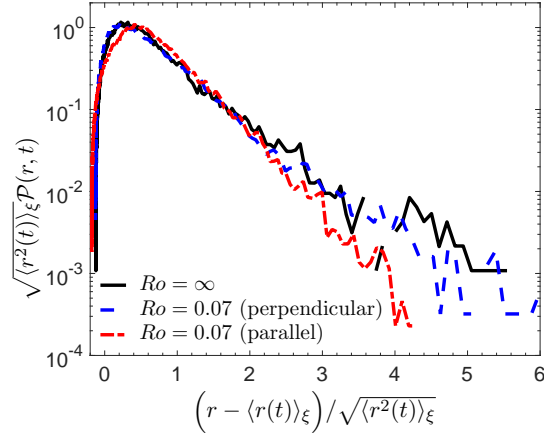


FIGURE 2. DNS results for $\mathcal{P}(r, t)$ for fluid particles with initial separation $\xi \in [1, 2]\eta$, plotted in standard form. The black solid line corresponds to the simulation without rotation $Ro = \infty$, for which the dispersion is isotropic, and the blue dashed and red dashed-dot lines correspond to dispersion in the directions perpendicular and parallel to the rotation axis, respectively, for a flow with $Ro = 0.07$.

forces in the particle equation of motion were switched off). In these simulations, the inertial particles are first run until their statistics reach a stationary state. We then store the particle trajectories and construct $\langle r^2(t) \rangle_\xi$ via a postprocessing step wherein we search for particles with separation ξ and then use these identified trajectories to compute $\langle r^2(t) \rangle_\xi$. The results therefore represent the particle multiscale dispersion properties in the steady state where the effects of the initial particle velocities (which were set equal to the local fluid velocity) become irrelevant.

The results for $\langle r^2(t) \rangle_\xi$ from this simulation are shown in Figure 3. The results differ dramatically from known results for inertial particle dispersion in isotropic turbulence. In particular, in isotropic turbulence, $\langle r^2(t) \rangle_\xi$ grows faster as St is increased when ξ is in the dissipation range (Bec *et al.* 2010; Bragg *et al.* 2016). This behavior is associated with the formation of “caustics”, wherein inertial particles approach one another at small separations with large relative velocities (Wilkinson & Mehlig 2005). However, the results in Figure 3 show that $\langle r^2(t) \rangle_\xi$ grows more slowly as St is increased, implying that the inertial particle relative velocities at the small scales are smaller than those of fluid particles, and therefore the absence of caustics. This again may be caused by the effect of negative loops in the autocorrelation of $\Delta \mathbf{u}^p(t)$ for particles in rotating turbulence, but needs further investigation.

5. Conclusions

We have reported preliminary results on the multiscale motion of inertial particles in rotating turbulence. In general, the relative motion of particles in rotating turbulent flows is affected in two ways: first, directly, through Coriolis and centrifugal forces on the particles, and second, indirectly, since the turbulence transporting the particles is itself strongly modified by the rotation. We considered dispersion of both fluid and inertial particles in directions parallel and perpendicular to the rotation axis. We also derived new asymptotic predictions for dispersion in the perpendicular (normal to the rotation axis) direction, using Zeman phenomenology to describe the fluid velocity increment

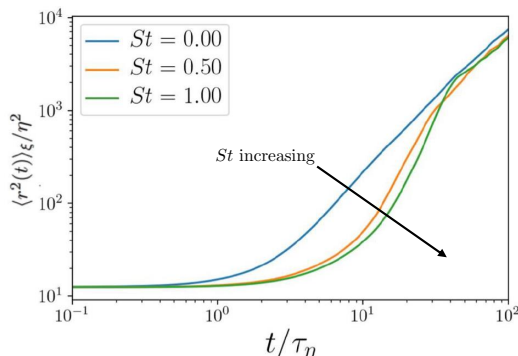


FIGURE 3. DNS results for $\langle r^2(t) \rangle_\xi$ for particles with different St . In this simulation, the fluid flow is subject to rotation with $Ro = 0.07$, however, in the particle equation of motion the Coriolis and centrifugal terms are switched off in order to investigate the implicit effects of rotation.

scaling. The mean-square separation results for fluid particles show that the dispersion is much stronger in the perpendicular than in the parallel direction, due to the quasi-two-dimensionalization of the flow at large scales. The theoretical predictions for the particle dispersion in the perpendicular direction did not match our DNS results; in fact, the DNS results showed that the perpendicular dispersion is very similar to the dispersion in the non-rotating case. This result is in part due to limited Zeman scaling for the fluid velocity increments in our DNS due to the moderate Reynolds number. However, it may be also due to rotation leading to strongly non-monotonic behavior in the Lagrangian autocorrelations of the fluid velocity increments. The results for the PDF of the fluid particle separation showed that the extreme events in the perpendicular direction are weakly affected by rotation, whereas the extreme events in the parallel direction are suppressed. We also obtained some preliminary results for the dispersion of inertial particles, where the direct effect of rotation were switched off. The mean-square dispersion results for inertial particles showed that the particles separate more slowly as St is increased. These results are dramatically different from those observed in non-rotating turbulence, where inertia is known to strongly enhance small-scale relative dispersion due to the effect of caustics. This may again be due to rotation leading to strongly non-monotonic behavior in the autocorrelations of the fluid velocity increments along the particle trajectories.

These preliminary results reveal some surprising effects of rotation on the multiscale motion of particles in turbulence. Many questions remain which shall be addressed in future work.

Acknowledgments

We gratefully acknowledge helpful suggestions from members of the Multiphase Flow group at the 2018 Summer Program.

REFERENCES

- BALESTRIN, E., DECKER, R., NORILER, D., BASTOS, J. & MEIER, H. 2017 An alternative for the collection of small particles in cyclones: Experimental analysis and CFD modeling. *Separation and Purification Technology* **184**, 54 – 65.

- BEC, J., BIFERALE, L., LANOTTE, A. S., SCAGLIARINI, A. & TOSCHI, F. 2010 Turbulent pair dispersion of inertial particles. *J. Fluid Mech.* **645**, 497–528.
- BIFERALE, L., BONACCORSO, F., MAZZITELLI, I. M., VAN HINSBERG, M. A. T., LANOTTE, A. S., MUSACCHIO, S., PERLEKAR, P. & TOSCHI, F. 2016 Coherent structures and extreme events in rotating multiphase turbulent flows. *Phys. Rev. X* **6**, 041036.
- BRAGG, A. & COLLINS, L. 2014 New insights from comparing statistical theories for inertial particles in turbulence: II. relative velocities of particles. *New J. Phys.* **16**, 055014.
- BRAGG, A., IRELAND, P. & COLLINS, L. 2016 Forward and backward in time dispersion of fluid and inertial particles in isotropic turbulence. *Phys. Fluids* **28**, 013305.
- BRAGG, A., SWAILES, D. C. & SKARTLIEN, R. 2012 Drift-free kinetic equations for turbulent dispersion. *Phys. Rev. E* **86**, 056306.
- BRAGG, A. D. 2017 Analysis of the forward and backward in time pair-separation probability density functions for inertial particles in isotropic turbulence. *J. Fluid Mech.* **830**, 63–92.
- CSANADY, G. T. 1973 *Turbulent Diffusion in the Environment*. Reidel, Boston.
- DAVIDSON, P. A. 2013 *Turbulence in Rotating, Stratified and Electrically Conducting Fluids*. Cambridge University Press.
- DEL CASTELLO, L. & CLERCX, H. J. H. 2011 Lagrangian acceleration of passive tracers in statistically steady rotating turbulence. *Phys. Rev. Lett.* **107**, 214502.
- ELPERIN, T., KLEEORIN, N. & ROGACHEVSKII, I. 1998 Dynamics of particles advected by fast rotating turbulent flow: Fluctuations and large-scale structures. *Phys. Rev. Lett.* **81**, 2898–2901.
- IRELAND, P. J., BRAGG, A. D. & COLLINS, L. R. 2016 The effect of reynolds number on inertial particle dynamics in isotropic turbulence. part 2. simulations with gravitational effects. *J. Fluid Mech.* **796**, 659–711.
- IRELAND, P. J., VAITHIANATHAN, T., SUKHESWALLA, P. S., RAY, B. & COLLINS, L. R. 2013 Highly parallel particle-laden flow solver for turbulence research. *Comput. Fluids* **76**, 170–177.
- MAXEY, M. R. & RILEY, J. J. 1983 Equation of motion for a small rigid sphere in a nonuniform flow. *Phys. Fluids* **26**, 883–889.
- PEKUROVSKY, D. 2012 P3DFFT: A framework for parallel computations of Fourier transforms in three dimensions. *SIAM J. Sci. Comput.* **34** (4), C192–C209.
- RICHARDSON, L. F. 1926 Atmospheric diffusion shown on a distance-neighbour graph. *Proc. R. Soc. London Ser. A* **110**, 709–737.
- ROTUNNO, R. & BRYAN, G. H. 2012 Effects of parameterized diffusion on simulated hurricanes. *J. Atmos. Sci.* **69**, 2284–2299.
- TOSCHI, F. & BODENSCHATZ, E. 2009 Lagrangian properties of particles in turbulence. *Annu. Rev. Fluid Mech.* **41**, 375–404.
- WILKINSON, M. & MEHLIG, B. 2005 Caustics in turbulent aerosols. *Europhys. Lett.* **71**, 186–192.
- ZAICHIK, L. I. & ALIPCHENKOV, V. M. 2009 Statistical models for predicting pair dispersion and particle clustering in isotropic turbulence and their applications. *New J. Phys.* **11**, 103018.
- ZEMAN, O. 1994 A note on the spectra and decay of rotating homogeneous turbulence. *Phys. Fluids* **6**, 3221–3223.